Available online at www.sciencedirect.com

SciVerse ScienceDirect

Ceramics International 39 (2013) 8253–8259

CERAMICS INTERNATIONAL

www.elsevier.com/locate/ceramint

Ballistic performance of liquid-phase sintered silicon carbide

Che-Yuan Liu[a], Wei-Hsing Tuan[a,*], Shih-Chieh Chen[b]

[a]Department of Materials Science and Engineering, National Taiwan University, Taipei, Taiwan
[b]Department of R&D, Hocheng Co., Taoyuan, Taiwan

Received 25 February 2013; received in revised form 11 March 2013; accepted 3 April 2013
Available online 10 April 2013

Abstract

The ballistic performances of liquid-phase sintered silicon carbide (SiC) specimens prepared by pressureless sintering were evaluated. Solid-state sintering additives were also used in preparation of additional SiC specimens for comparison purposes. SiC specimens prepared by adding solid-state sintering additives were also prepared for the purpose of comparison. With the addition of 10–15 wt% of Al_2O_3 and Y_2O_3, the strength and toughness of the liquid-phase sintered SiC (LSC) were higher than those of solid-state sintered SiC (SSC). Nevertheless, the hardness of LSC specimen tended to be lower. However, LSC specimens sintered at 1875 °C can pass the NIJ Level IV test. The microstructure observation provides direct evidence of the importance of hardness and toughness regarding ballistic performance. A performance index, the hardness/density ratio, is proposed to rank the ballistic performance on ceramics used for personnel armor applications.

Keywords: A. Sintering; C. Mechanical properties; D. SiC; E. Armor

1. Introduction

In order to neutralize ballistic impact energy, ceramics are often used in armor applications [1–6]. Although the mechanical properties, hardness, strength and toughness of ceramics are all important to evaluate the ballistic performance of ceramics, a recent study has raised doubt in regards to the role of toughness on ballistic performance [6]. The resistance of ceramics under ballistic attack involves complex interactions between the ceramics and projectiles. Until now, no single parameter has been considered satisfactory for defining the ballistic performance of ceramics.

The most popular ceramics for armor are alumina (Al_2O_3) and silicon carbide (SiC). Boron carbide (B_4C) has also been considered as a potential ceramic for armor due to its low density. However, the resistance of B_4C specimens under multi-hits is rather disappointing [7]. Moreover, since the density of Al_2O_3 is relatively high, SiC has received wider attention for its use as body armor. Due to certain covalent bonding characteristics, the densification of bulk SiC via pressureless sintering is possible only when several sintering aids are used. Furthermore, after the addition of solid-state sintering additives, such as boron and carbon, the full densification of SiC is only possible when the sintering temperature is higher than 2000 °C [8]. However, the extremely high sintering temperature imposes a high cost on the SiC products. The addition of liquid-phase sintering additives offers a promising solution because they allow the sintering temperature to be reduced. However, this benefit is traded off with a decrease in hardness [9]. The use of liquid-phase sintered SiC as armor plate thus needs to be evaluated in order to determine whether they are suitable alternatives to solid-state sintered SiC.

Evaluation of the ballistic performance of various ceramics is a challenging task, however. Although several indexes, such as hardness, toughness etc., have been proposed to evaluate the ballistic performance of ceramics for armor application, the use of these indexes on liquid-phase sintered SiC has not yet been employed.

Most SiC armor specimens are prepared by a hot-pressing technique [10]. This technique limits the size and shape of armor specimens. In order to improve the economic feasibility of SiC specimen preparation, the use of pressureless sintering is important. In the present study, a liquid-phase, Y_2O_3–Al_2O_3–SiO_2, was used to assist the densification of the SiC.

*Corresponding author. Tel.: +886 2 33663899; fax: +886 2 23659800.
E-mail address: tuan@ntu.edu.tw (W.-H. Tuan).

0272-8842/$ - see front matter © 2013 Elsevier Ltd and Techna Group S.r.l. All rights reserved.
http://dx.doi.org/10.1016/j.ceramint.2013.04.010

The mechanical properties of the liquid-phase sintered SiC were determined. The ballistic performance of the SiC was then evaluated. Some solid-state sintered SiC specimens were also prepared for the purpose of comparison. A performance index was then proposed to rank their ballistic performance.

2. Experimental procedures

The SiC content in the starting silicon carbide powder (UF-15, H.C. Starck Co., Germany) used in the present study was higher than 98%. The average particle size of the SiC powder was 0.55 μm and the crystalline phase was α-phase. The liquid phase sintering aids were Al_2O_3 (AL-160SG-4, Showa Denko Co., Japan) and Y_2O_3 (Ganzhou Deshipu Advanced Material, China) powders; the average particle sizes of the powders were 0.55 μm and 3.5 μm, respectively. The amount of the liquid-phase sintering aids per specimen was 10 wt% or 15 wt%. The weight ratio of Al_2O_3 to Y_2O_3 was 2:3. Table 1 shows the compositions for all the specimens prepared in the present study.

The powder mixtures were milled in deionized water for 3 h using SiC grinding media. A binder, polyvinyl alcohol (PVA), with 1 wt% was added during milling. The drying process was carried out with a spray dryer. Green powder compacts, with the dimensions of 58 × 58 × 11.5 mm, were prepared by die-pressing at a uniaxial pressure of 130 MPa. The green body was pre-fired at 600 °C for 1 h in air to remove the binder. The sintering was then conducted in a graphite furnace within a temperature range from 1850 °C to 1900 °C in a flowing argon. The crucible used was also graphite. The heating rate was 5 °C/min from room temperature to 1800 °C, and 2.5 °C/min from 1800 °C to the sintering temperature. The dwell time at sintering was 1 h. The density of the sintered specimens was determined using Archimede's method. The crystalline phase was identified using X-ray diffraction technique (D2 Phaser, Bruker Co., Germany). Since specimens prepared using liquid-phase sintering additives and densification at 1875 °C could pass the ballistic test, the microstructure and properties for these specimens were determined, which are illustrated, unless otherwise stated.

Some silicon carbide specimens were prepared by adding the solid-state sintering aids boron (Grade I, H.C. Starck Co., Germany) and carbon (14029-U, Sigma-Aldrich Chemie GmbH, Germany). The total amount of boron and carbon was 1.5 wt%, as shown in Table 1. The powder preparation procedures were the same as for the liquid-phase sintered specimens. The heating rate was 5 °C/min from room temperature to 1800 °C and 1.5 °C/min from 1800 °C to 2050 °C. The dwell time at 2050 °C was 1 h.

Table 1
Notation and starting compositions for the SiC specimens prepared in the present study.

Specimens	SiC/wt%	*B*/wt%	*C*/wt%	Al_2O_3/wt%	Y_2O_3/wt%
SSC	98.5	1.2	0.3	–	–
LSC10	90.0	–	–	4.0	6.0
LSC15	85.0	–	–	6.0	9.0

A four-point bending technique was used to determine the flexural strength with a universal testing machine (Micro350, Testometrix Co., UK). The cross-head speed was 0.5 mm/min. The dimensions of the testing bars were 3 × 4 × 50 mm. The upper and lower spans were 10 mm and 30 mm. The surface of the testing bar was ground in the longitudinal directions with diamond wheels. After polishing with diamond pastes, the Vickers hardness and fracture toughness were measured with the indentation technique (FM-700, Nakazawa Co., Japan). The load applied was 9.8 N. At least 15 measurements were made for each average value. The relationship proposed by Chantikul et al. was used to calculate the fracture toughness [11]. The elastic modulus was determined via the ultrasonic method set to 5 MHz (pulse receiver 5055PR and oscilloscope 9354CM, LeCroy Co., New York). Microstructure observation on the fracture and polished surfaces was conducted using scanning electron microscopy (JEOL 5400, JEOL Co., Japan).

For the ballistic testing, several SiC specimens were joined together with resin and backed with Twaron™ fibers. The thickness of the backing fibers was 4.5 mm. The final dimensions of ballistic testing panels were 250 × 300 × 14 mm. The testing procedures followed the National Institute of Justice Standard (NIJ) 0108.01. The projectiles used for the ballistic testing were 0.30 WC-Co-core armor piercing (AP) bullets. Their speed was 868 ± 15 m/s. Four to six panels were used for each composition or each sintering condition.

3. Results

The density of the SiC specimens after pressureless sintering is shown in Table 2. The mechanical properties, hardness, elastic modulus, flexural strength and toughness are also shown. Comparing the properties of the SSC and LSC specimens, the strength and toughness of LSC specimens were respectively 15–70% and 40–70% higher than those of the SSC specimens. However, the hardness of LSC specimens was 10–30% lower than that of SSC specimens.

A typical micrograph for the liquid-phase sintered silicon carbide (LSC) specimen is shown in Fig. 1. The amount of starting liquid-phase sintering additives in the specimen was 10 wt%. After sintering at 1875 °C for 1 h, the SiC grains had become slightly elongated with a grain size around 2 μm. The amount of second phase in the sintered specimen was around 20 vol%. Fig. 2 shows the XRD patterns for the sintered SSC and LSC specimens. For the solid-state sintered specimens (SSC), the SiC-polytypes 6H, 15R and 4H were detected. A very small amount of graphite was also found. For the liquid-phase sintered specimens (LSC), the SiC-6H, 15R, 4H and several second phases were detected. For the LSC specimen sintered at 1850 °C, the second phases were mainly composed of yttria-alumina-garnet (YAG, $3Y_2O_3$–$5Al_2O_3$, $Y_3Al_5O_{12}$), yttria-alumina-monoclinic (YAM, $2Y_2O_3$–Al_2O_3, $Y_4Al_2O_9$) and $AlY_3C_{0.5}$. Apart from these second phases, the glassy phase, Y_2O_3–Al_2O_3–SiO_2 silicate, remained in the LSC specimens. The presence of such a non-crystalline phase

Table 2
Sintering conditions for the SiC specimens and their properties.

	Sintering temp./°C	Density/g/cm^3	Vickers hardness/GPa	Elastic modulus/GPa	Flexural strength/MPa	K_{IC}/MPam$^{0.5}$	Sonic velocity/m/s	D value/10^{12} s^{-1}
SSC	2050	3.05 ± 0.05	23.2 ± 0.1	387	317 ± 23	2.7 ± 0.3	11.5	5.1
LSC10	1850	3.14 ± 0.01	17.7 ± 1.8	377	482 ± 30	4.4 ± 0.4	11.4	1.4
LSC10	1875	3.22 ± 0.01	20.1 ± 0.5	396	537 ± 62	4.2 ± 0.6	11.5	1.9
LSC10	1900	3.15 ± 0.03	19.0 ± 3.5	395	465 ± 94	3.8 ± 0.5	11.7	2.2
LSC15	1850	3.20 ± 0.01	15.6 ± 2.6	370	365 ± 30	4.6 ± 0.7	11.2	1.1
LSC15	1875	3.27 ± 0.02	18.6 ± 0.2	381	473 ± 78	4.5 ± 0.3	11.3	1.4
LSC15	1900	3.25 ± 0.03	18.0 ± 1.5	391	403 ± 83	4.2 ± 0.6	11.4	1.6

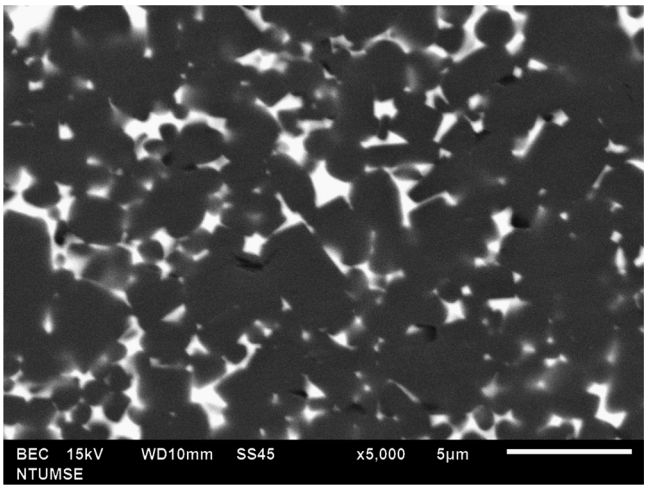

Fig. 1. Microstructure of a typical liquid-phase sintered silicon carbide (LSC). The specimen contained 10 wt% sintering aids and sintered at 1875 °C.

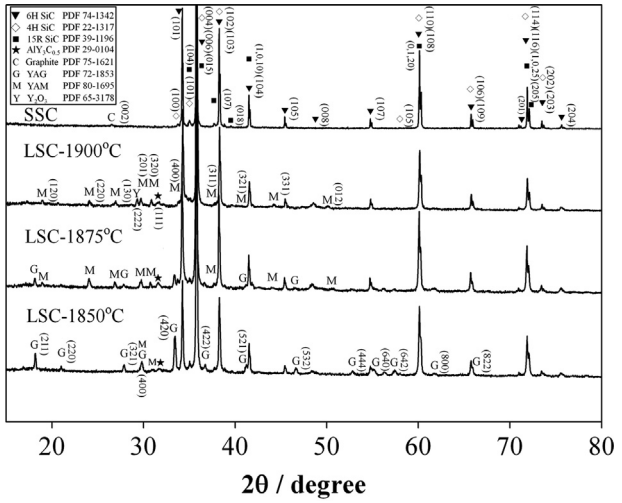

Fig. 2. XRD patterns for the SSC specimen sintered 2050 °C, LSC10 specimens sintered at 1850 °C, 1875 °C and 1900 °C.

reduces the sintering temperature from 2050 °C to 1875 °C. The YAG and YAM phases were the precipitates from the liquid phase during the cooling stage [12]. The second phase in the LSC specimen sintered at 1850 °C was mainly YAG phase. With the increase of sintering temperature, the amount of YAG became consumed by the increase of YAM. For the LSC specimen sintered at 1900 °C, YAG phase was hardly observed and a small amount of Y_2O_3 was detected. The peak height of the second phases in the XRD patterns indicated that the amount of crystalline second phase decreased with the increase of sintering temperature and that the liquid increased with the increase of sintering temperature.

Fig. 3 shows the interactions between a crack induced by Vickers indentation and the SiC grains. For the liquid-phase sintered specimen (Fig. 3a), the crack mainly propagated along the boundary phase. For the solid-state sintered specimen, the crack path was straight, which suggests that the crack penetrated through the grains (Fig. 3b).

Table 3 shows the ballistic test results. All the SSC specimens passed the NIJ Level IV test. The heights of all bulges at the back of specimen panels were measured. The height of the bulge at the back of the SSC panels was around 13 mm. For the LSC specimens, the AP projectiles penetrated through the LSC panels for the specimens sintered at 1850 °C. The LSC specimens prepared by sintering at 1875 °C passed the NIJ Level IV test. The height of the bulge at the back of the LSC panels varied from 13 to 16 mm, depending on the amount of liquid-phase sintering additives. Since the hardness, strength and toughness of the LSC specimens prepared by sintering at 1900 °C were all lower than those of the specimens prepared at 1875 °C (see Table 2) these were not used for the ballistic test.

Fig. 4 shows the remains of the AP projectiles before and after ballistic tests. After each ballistic test, the debris of the projectile was collected. The heads of the AP projectiles were shattered into small fragments. There was a strong correlation between hardness and the fracturing behavior of projectiles. The AP projectile broke into smaller fragments as the hardness of SiC specimens increased. The hardness of the SSC specimens was higher than that of the LSC specimens. The hardness of the LSC10 specimen was higher than that of the LSC15 specimen, which must be due to a lower liquid phase content in LSC10.

By removing the cover fiber layer, the remains of the SiC specimens after the ballistic test were observed. Fig. 5 shows the morphology of the LSC10 and SSC specimens in the panels after ballistic tests. For the LSC panel, only the specimen under attack was broken (Fig. 5a). The nearby

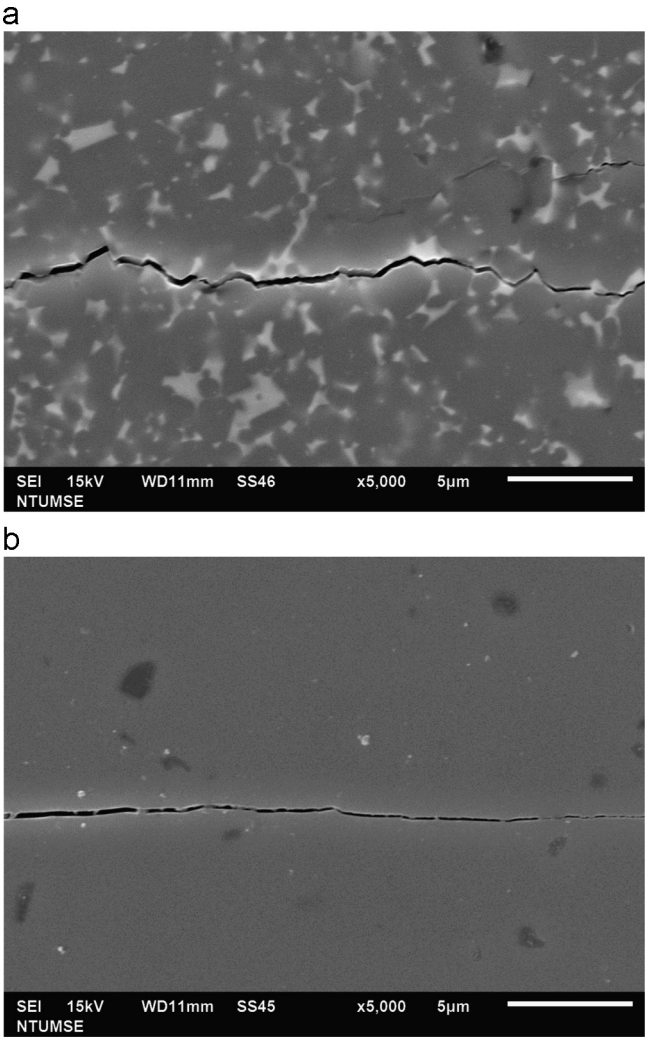

Fig. 3. Interactions between SiC grains and indentation-induced crack in the (a) LSC10 and (b) SSC specimens.

Table 3
Ballistic testing results for the SiC panels prepared in the present study.

Specimen	No. of projectiles used	No. of penetrations	Bulge of backing material/mm	NIJ Level IV test
SSC	5	0	13.2 ± 1.3	Pass
LSC10-1850	4	4	–	Fail
LSC10-1875	6	0	13.3 ± 1.8	Pass
LSC15-1850	4	4	–	Fail
LSC15-1875	5	0	15.5 ± 2.4	Pass

specimens were intact. For the SSC specimens, not only the specimen under strike by the AP projectile was broken, but the nearby SSC specimens were also broken (Fig. 5b). The LSC and SSC panels were assembled with the same resin and procedures. The LSC specimens seem to absorb more energy from the attack. The nearby LSC specimens were not affected. This result demonstrates that the resistance of the LSC specimens under multiple hits is likely higher.

Fig. 6 shows the typical fracture surface of the broken pieces collected from the SiC specimens after ballistic tests. The fracture mode of the LSC specimen is mainly an inter-granular one (Fig. 6a) while the fracture of the SSC specimen is a trans-granular one (Fig. 6b). The fracture path induced by indentation in fig. 3 is the same as that shown in fig. 6. This demonstrates that the fracture mode produced by relatively slow crack growth (via Vickers indentation) is similar to that produced by fast crack growth (via ballistic attack).

4. Discussion

In the present study, the silicon carbide specimens were prepared using solid-state sintering additives, boron and carbon, as well as liquid-phase sintering additives, Y_2O_3 and Al_2O_3. The lowest eutectic temperature for the Y_2O_3–Al_2O_3–SiO_2 system is around 1400 °C [13]. A liquid phase is thus formed when the sintering is conducted above 1850 °C. A weight loss around 7% was observed after pressureless sintering in the graphite furnace. Such weight loss has been reported for the pressureless sintering of the Y_2O_3–Al_2O_3–SiC system [13–15], and results from the vaporization of SiO, CO and Al_2O during sintering. Although such weight loss occurs, however, the density of the LSC specimens became higher than 3.2 g/cm^3 when the sintering temperature was higher than 1875 °C. Furthermore, the sonic velocity of the ultrasonic wave (Table 2) in the LSC specimen was close to that of the SSC specimens. The sensitivity of the sonic velocity to the amount of pores within the specimens suggests that the porosity in the LSC specimens must be close to that of the SSC specimens. By assuming that the theoretical density of the solid-sintered SiC is 3.21 g/cm^3 [16], the relative density of the SSC specimens should be $94.9 \pm 1.6\%$, which is a value confirmed by the micrographs shown in Figs. 3(b) and 6(b). The relative density of the LSC specimens must therefore be close to 95%. This value can also be confirmed via the observation of the LSC microstructure. A typical micrograph for the LSC10 specimen is shown in Fig. 1. The porosity in this micrograph is less than 5 vol%. This demonstrates that the dense SiC armor-specimens can be prepared by using pressureless sintering through the use of liquid-phase sintering aids such as Y_2O_3 and Al_2O_3. The weight loss of LSC specimens, possibly due to vaporization prior to densification, causes little problem to the densification of the LSC specimens.

The reaction phases for the Y_2O_3–Al_2O_3–SiO_2 system are mainly $Y_3Al_5O_{12}$ (YAG), $Y_4Al_2O_9$ (YAM) and $Y_2Si_2O_7$ [13]. Apart from the liquid phase, the YAG and YAM phases are also found in the sintered specimens. The absolute density of these reaction phases is higher than that of SiC. The absolute density of the LSC specimen must therefore be higher than that of the SSC specimen. Nevertheless, the amount of porosity in the LSC specimens should be close to that found in the SSC specimens.

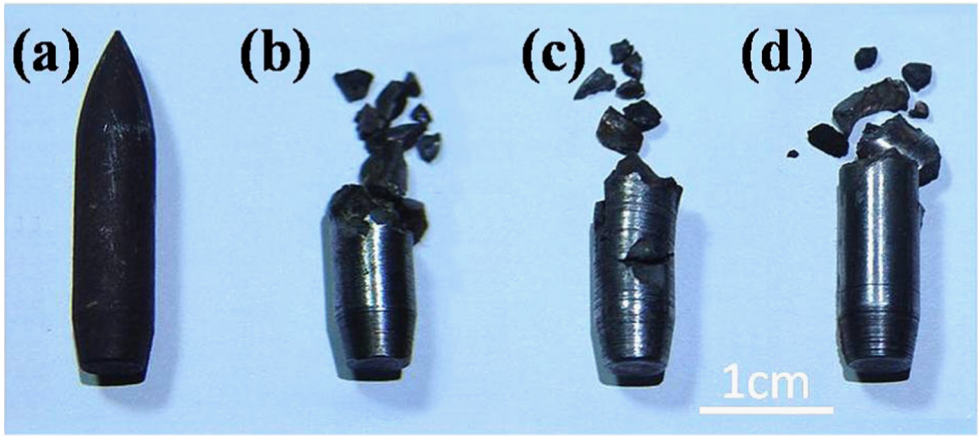

Fig. 4. Projectile (a) before and after hitting the (b) SSC, (c) LSC10 and (d) LSC15 panels.

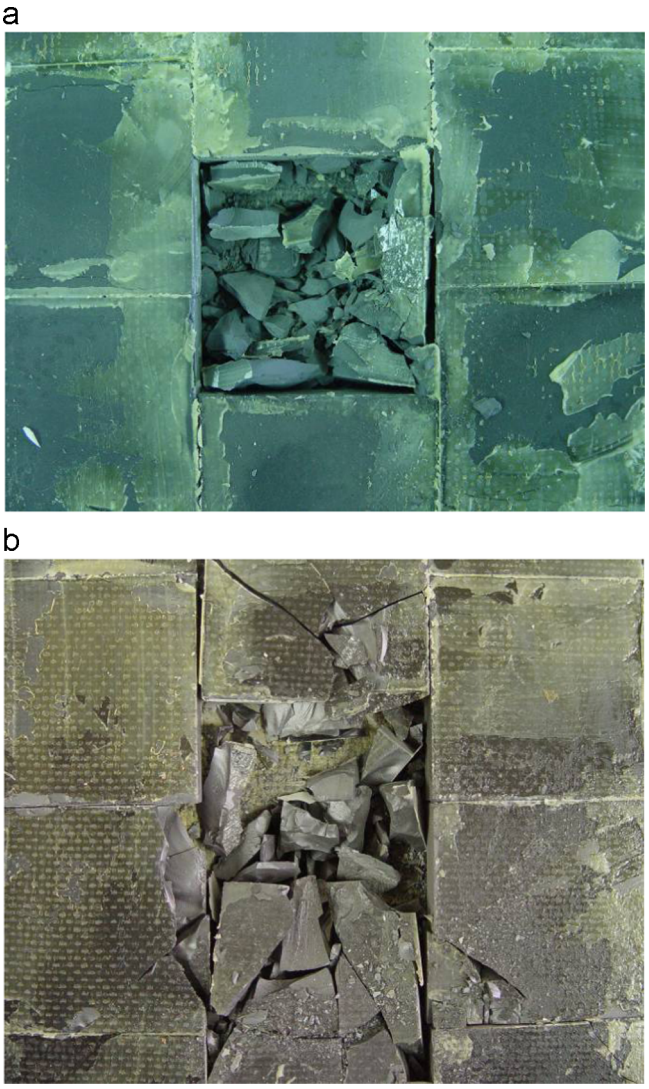

Fig. 5. (a) LSC10 and (b) SSC specimens in the panels after ballistic test.

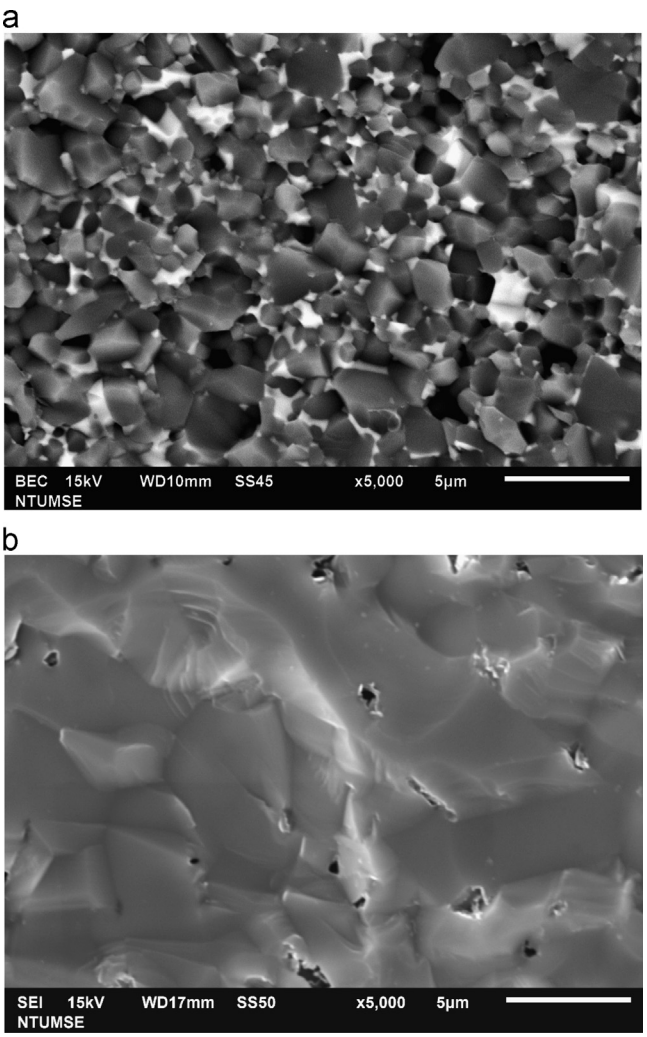

Fig. 6. Fracture surfaces of (a) LSC10 and (b) SSC specimens after ballistic test.

The mechanical properties for all the specimens are shown in Table 2. With the addition of liquid phase sintering additives, the flexural strength and toughness of SiC are enhanced. However, the Vickers hardness is reduced. There has been a long-standing pursuit for an index to evaluate the ballistic performance of various ceramics. An index known as

the ballistic energy dissipation criterion (D) has been frequently used to evaluate the ballistic performance [17]. This index combines several mechanical properties of the ceramic as

$$D = 0.36\frac{H_v E C}{K_{IC}{}^2} \quad (1)$$

In the above equation, the H_v is the Vickers hardness, E the elastic modulus, C the sonic velocity and K_{IC} the fracture toughness. The values for D are also shown in Table 2. The toughness is enhanced by 50% after the addition of liquid phase, so the D values drop significantly. Judging from the D values, the ballistic performance of SSC specimens should be much better than that of LSC specimens. However, from the bulge height at the back of the armor panel (Table 3), the ballistic performance in SSC specimens appears only slightly better than that of the LSC specimens. Furthermore, the LSC specimens exhibit a better resistance to multiple hits (Fig. 5). This implies that the fracture behavior during ballistic attacks is complex. Therefore, there is a need to define an index to correlate the ballistic performance and material properties.

The morphology of the AP projectiles after hitting each SiC specimen (Fig. 4) suggests that the hardness of ceramic specimens plays an important role in ballistic performance. For harder ceramic specimens, more bullet debris is produced after hitting the ceramic. Smaller debris imposes less threat to the brittle ceramics. The higher hardness is therefore preferred. Table 2 demonstrates that when the hardness is higher than 18 GPa, the SiC specimens can pass the NIJ level IV test. This suggests that the hardness alone is useful enough to rank the SiC specimens. For example, the LSC specimen that sintered at 1850 °C fails to pass the NIJ IV test due to its lower hardness; and thus can be considered lower in rank than that of the LSC specimen sintered at 1875 °C that passed the test.

The fracture mode reflects the amount of energy dissipation during the fracture process. More energy is needed to produce a higher degree of fracture across the surface. The thermal expansion mismatch between SiC and liquid-phase induced second phase (thermal expansion coefficient of YAM and YAG$\sim 8\times10^{-6}$/°C, of SiC$\sim 4.5\times10^{-6}$/°C [18]) produces stresses at the grain boundaries. The crack thus tends to propagate along the grain boundaries regardless of the crack propagation speed. The LSC specimen exhibits higher toughness due to its fracture mode being inter-granular. Although the role of fracture toughness on ballistic performance is currently under debate [6,19,20], by comparing Figs. 4 and 6, it becomes clear that the fracture mode for the SiC specimens is the same under slow crack growth (Vickers indentation) versus under fast crack growth (bullet hitting). This thus implies that the fracture toughness is a useful index to show the interaction between SiC grains and cracks. It is also interesting to note the weight of the fracture toughness on the value of D (Eq. (1)). The square of the toughness in the equation suggests that the role of toughness on the ballistic performance is important. However, the value of D fails to shed light on the observation that the ballistic performance of LSC is close to that of SSC. From the morphology of the SiC panels after ballistic tests (Fig. 5), the toughness indeed appears to be an important parameter. This reflects the fact that there is resistance in the ceramic material to the fracture of the nearby SiC specimen. As the SiC specimen can absorb more energy under attack, less energy can pass on to the next SiC specimen. The nearby SiC specimen can then survive to defeat the next ballistic threat. Therefore, toughness is a useful index for body armor under multiple attacks.

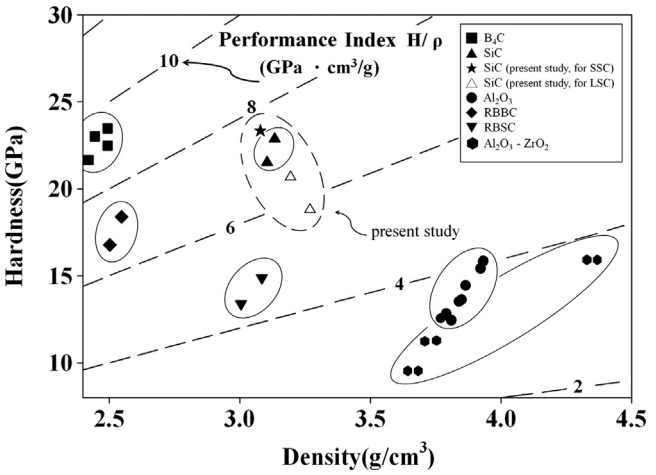

Fig. 7. Density vs. hardness for various armor ceramics. The dotted lines show the performance index. Along with our experimental data, the data reported from the Medvedovski's papers [17] are also shown.

There are many ceramics available for armor application. A justified parameter is needed for choosing a suitable ceramic. Prof. Ashby has developed a conceptual tool to guide the material selection [21]. The tool uses performance indices to describe material performance. As discussed above, the weight is an important consideration for personnel armor, with a lower density being preferred. Likewise, hardness is another important factor. Since both hardness and density are important parameters to evaluate the ballistic performance of ceramics, we propose a performance index, the hardness/density ratio, to rank the ballistic performance of ceramics for body armor application. The values of the hardness/density ratio for the LSC and SSC specimens are shown in Fig. 7. The data reported for other armor ceramics [17] were also collected and shown in the figure. These data include the reported values for silicon carbide. Our experimental values are close to the reported values. The figure shows the performance index values of the SSC specimens are indeed slightly higher than that of LSC specimens.

The hardness/density ratio serves as a straightforward index to rank the ceramics for armor application. Fig. 7 demonstrates that the ballistic performance of SiC is better than that of many other ceramics, such as alumina and reaction bonded silicon carbide (RBSC). However, this index only takes density and hardness into account. The influence of toughness is not included. Since the toughness may affect the ballistic performance under multiple attacks, further study on the evaluation of factors affecting multiple attacks is still needed.

5. Conclusions

Several conclusions can be made from the experimental results presented in the present study:

1. The liquid-phase sintered SiC prepared through pressureless sintering can be used as body armor.
2. The hardness of ceramics is critical to ballistic resistance. The projectile is fractured into smaller pieces after hitting a harder ceramic. Smaller debris imposes less threat.
3. The toughness may play an important role on the ballistic performance under multiple attacks. However, more experimental data are needed to identify the key material characteristic of such resistance.
4. The hardness/density ratio is a useful performance index to rank the ballistic performance. This index demonstrates that the ballistic performance of solid-state sintered SiC is slightly superior to that of liquid-phase sintered SiC. Moreover, the ballistic resistance of SiC is better than many ceramics, such as alumina, RBSC etc.

Acknowledgments

The technical help from colleagues of the Dept. of R&D, Hocheng Co., was very supportive. The financial support from the Economic Ministry of Taiwan under Contract no. of 95-EC-17-A-01-I1-0037 is appreciated.

References

[1] B. Mikijelj, M. Chheda, J. Shih, H. Knoch, Light weight ceramic armor-influence of processing on ballistic performance, Advances in Science and Technology 45 (2006) 1729–1738.
[2] M. Tian, G. Yan Zili1, Z. Jianmin, Zhonglei, Z. Jianchun, Microhardness of various bullet-proof ceramics, Advanced Materials Research 177 (2011) 154–156.
[3] R.G. O'Donnell, An investigation of the fragmentation behaviour of impacted ceramics, Journal of Materials Science Letters 10 (1991) 685–688.
[4] R.G. O'Donnell, Fragmentation of ceramics in armour, Journal of Materials Science Letters 11 (1992) 1227–1230.
[5] Z. Rozenberg, Y. Yeshurun, The relation between ballistic efficiency and compressive strength of ceramic tiles, International Journal of Impact Engineering 7 (1988) 357–362.
[6] M. Flinders, D. Ray, A. Anderson, R.A. Culter, High-toughness silicon carbide as armor, Journal of the American Ceramic Society 88 (8) (2005) 2217–2226.
[7] M.W. Chen, J.W. McCauley, K.J. Hemker, Shock-induced localized amorphization in boron carbide, Science 299 (2003) 1563–1566.
[8] K. Biswas, Solid state sintering of SiC-ceramics, Materials Science Forum 624 (2009) 71–89.
[9] A. Gubernat, L. Stobierski, P. Labaj, Microstructure and mechanical properties of silicon carbide pressureless sintered with oxide additives, Journal of the European Ceramic Society 27 (2007) 781–789.
[10] P.G. Karandikar, G. Evans, S. Wong, M.K. Aghajanian, A review of ceramics for armor applications, Ceramic Engineering and Science Proceedings 29 (6) (2008) 163–175.
[11] P. Chantikul, G.R. Anstis, B.R. Lawn, D.B. Marshall, A critical evaluation of indentation techniques for measuring fracture toughness: I, Direct crack measurements, Journal of the American Ceramic Society 64 (1981) 533.
[12] N.P. Padture, In situ-toughened silicon carbide, Journal of the American Ceramic Society 77 (2) (1994) 519–523.
[13] A. Can, M. Herrmann, D.S. McLachlan, I. Sigalas, J. Adler, Densification of liquid phase sintered silicon carbide, Journal of the European Ceramic Society 26 (2006) 1707–1713.
[14] G. Magnani, L. Beaulardi, Luigi Pilotti, Properties of liquid phase pressureless sintered silicon carbide obtained without sintered bed, Journal of the European Ceramic Society 25 (2005) 1619–1627.
[15] T. Grande, H. Sommerset, E. Hagen, K. WiiK, M.A. Einnarsrud, Effect of weight loss on liquid-phase-sintered silicon carbide, Journal of the American Ceramic Society 80 (1997) 1047–1052.
[16] G.L. Harris, Properties of silicon carbide, EMIS Data Reviews Series N13 (1995) 3.
[17] E. Medvedovski, Ballistic performance of armour ceramics: influence of design and structure, Ceramics International 36 (2010) 2103–2115.
[18] D.H. Kim, C.H. Kim, Toughening behavior of silicon carbide with additions of yttria and alumina, Journal of the American Ceramic Society 73 (1990) 1431–1434.
[19] C.J. Shih, V.F. Nesterenko, M.A. Meyers, High-strain-rate deformation and comminution of silicon carbide, Journal of Applied Physics 83 (1998) 4660–4671.
[20] D. Ray, M. Flinders, A. Anderson, R.A. Culter, Effect of microstructure and mechanical properties on ballistic performance of SiC-based ceramics, Ceramic Engineering and Science Proceedings 27 (2008) 85–96.
[21] M.F. Ashby, Criteria for selecting the components of composites, Acta Metallurgica 41 (1993) 1313–1335.